HHS Public Access

Author manuscript

Am J Ophthalmol. Author manuscript; available in PMC 2016 June 01.

Published in final edited form as:

Am J Ophthalmol. 2015 June ; 159(6): 1169–1179.e2. doi:10.1016/j.ajo.2015.02.019.

Superior Oblique Extraocular Muscle Shape in Superior Oblique Palsy

Sun Young Shin, M.D.[1,6] and **Joseph L. Demer, M.D., Ph.D.**[1,2,3,4,5]

[1]Department of Ophthalmology, David Geffen Medical School at University of California, Los Angeles

[2]Stein Eye Institute, David Geffen Medical School at University of California, Los Angeles

[3]Department of Neurology, David Geffen Medical School at University of California, Los Angeles

[4]Neuroscience, David Geffen Medical School at University of California, Los Angeles

[5]Bioengineering Interdepartmental Programs, David Geffen Medical School at University of California, Los Angeles

[6]Department of Ophthalmology and Visual Science, Seoul St. Mary's Hospital, College of Medicine, The Catholic University of Korea, Seoul, South Korea

Abstract

Purpose—To investigate the superior oblique (SO) extraocular muscle cross section in normal controls and in SO palsy using high-resolution magnetic resonance imaging (MRI).

Design—Prospective observational study.

Methods—At a single academic medical center, high resolution MRI was obtained at 312 micron in-plane resolution using surface coils in multiple, contiguous, quasi-coronal planes perpendicular to the orbital axis in 12 controls and 62 subjects with SO palsy. Previous strabismus surgery was excluded. Imaging was repeated in central gaze and infraduction. In each image plane along the

Address for Correspondence: Joseph L. Demer, M.D., Ph.D. ,Stein Eye Institute, 100 Stein Plaza, UCLA, Los Angeles, California, 90095-7002 U.S.A., Phone: 310-825-5931, Fax: 310-206-7826, jld@jsei.ucla.edu.

Contributions of Authors: Design of the study (SYS, JLD); Conduct of the study (SYS, JD); Collection, management, analysis, and interpretation of the data (SYS, JD); and Preparation, review, and approval of the manuscript (SYS, JD).

Financial Disclosures: Grant support as listed above. JLD is salaried as a full time professor of Ophthalmology and Neurology at UCLA, and holds the Leonard Apt Endowed Professorship in Pediatric Ophthalmology. JLD has received publication royalties from Karger Medical and Scientific Publishers. JLD has served as a consultant to the Pediatric Ophthalmology Investigators Group, the Division of Research Grants of the United States National Institutes of Health, the National Eye Institute Board of Scientific Counselors, and the Knights Templar Eye Foundation. JLD has received lecture honoraria from: Emory University, State University of New York Downstate, Columbia University, University of Michigan, American Academy of Pediatrics, North American Neuroophthalmological Society, European Ophthalmological Society, University of Houston, and Wake Forest University Medical Center. JLD has received travel support from the Australian Squint Club, Colombian Association for Pediatric Ophthalmology and Strabismus, European Ophthalmological Society, Goldschleger Eye Institute, and University of Cambridge.

SO, its cross section was outlined to compute cross sectional area and the major and minor axes of the best-fitting ellipse. Main outcome measures were SO morphology and ocular motility.

Results—The major and minor axes, cross sectional area distributions, and volume of the SO belly were subnormal in orbits with SO palsy at most anteroposterior locations (P=0.001), but discriminant analysis showed that palsied SO cross sections segregated distinctly into round and elongate shapes representing isotropic vs. anisotropic atrophy, respectively. The major axis was relatively preserved in anisotropic atrophy (P=0.0146). Cases with isotropic atrophy exhibited greater hypertropia in infraversion than central gaze, as well as greater exclyclotorsion, than cases with anisotropic atrophy (P<0.05 for all).

Conclusions—Characteristic differences in shape of the palsied SO belly correlate with different clinical features, and may both reflect the degree of differential pathology in the medial versus lateral neuromuscular SO compartments, and the basis for diversity in patterns of resulting hypertropia.

Introduction

Compartmentalization has been recognized recently as a feature of most extraocular muscles[1]. There is a selective pattern of terminal intramuscular motor innervation in horizontal rectus muscles[2,3], and the inferior rectus muscle[4]. The lateral rectus muscles of humans and monkeys consist of distinct superior and inferior muscle fiber compartments separately innervated by either a superior or inferior abducens nerve division[4,5]. This anatomical division of lateral rectus muscle into separate compartments has been correlated with multipositional magnetic resonance imaging (MRI) demonstrating differential contractility during ocular counter-rolling [6] and vertical fusional vergence[7]. The potential for transmission of differential forces in the two compartments to different insertional points on the globe has been demonstrated by biomechanical measurements showing mechanical independence of passive tensile forces in the compartments of bovine extraocular muscles[8,9] and tendons[10], as well as actively-generated forces in both the orbital and global layers, and transverse compartments, of bovine extraocular muscles[11]. The frequent occurrence of selective atrophy of the superior compartment of the lateral rectus[3] may be related to the observation of incomitant hypertropia in clinical unilateral lateral rectus weakness, which suggests selective compartmental paralysis or paresis[12].

Recently, Le et al. extended the theme of compartmentalization to the superior oblique (SO) muscle when they described in this muscle evidence for selective compartmental innervation (Le A, et al. IOVS 2014;55:ARVO E-Abstract 2559). The trochlear nerve bifurcates external to the SO belly into medial and lateral branches that innervate non-overlapping compartments of the muscle. The medial compartment inserts anteriorly near the globe equator and thus would have mechanical advantage favoring predominantly torsional action in central gaze, while the lateral compartment inserts posteriorly and would have mechanical advantage favoring a predominantly vertical action. The functional implications of this anatomic finding have been extended using MRI to differential compartmental functional of SO during vertical fusional vergence[7].

In both acquired and congenital SO palsy, MRI studies have shown the affected SO belly to be atrophic or hypoplastic [13–18]. Demer et al. reported marked reduction in midorbital cross section in denervated SO muscles in MRI and variable atrophy of muscle fiber following experimental intracranial trochlear neurectomy in monkey[18]. Atrophy of the SO belly therefore can be considered a finding sufficient to establish the diagnosis of SO palsy. We wondered if the SO impaired by a trochlear lesion might exhibit selective compartmental atrophy similar to the lateral rectus and if so, supposed that the clinical effects of selective compartmental SO palsy might differ from complete palsy. However, no study has attempted to examine the shape of atrophied SO belly in MRI as yet.

Therefore, this study sought to investigate, using high-resolution MRI in a large number of cases, possible variations in the morphologic pattern of SO atrophy, and their relationship to clinical characteristics of SO palsy.

Methods

Subjects

This prospective, observational study was conducted at Stein Eye Institute, a single academic medical center at the University of California, Los Angeles (UCLA). Volunteers gave written, informed consent according to a protocol approved by the UCLA Institutional Review Board that conformed to the tenets of the Declaration of Helsinki. We studied a control group of 12 normal, orthotropic volunteers recruited by advertisement of mean (± standard deviation, SD) age 46.2±18.3 (range, 14–61) years; there were 5 men and 7 women. Each control underwent comprehensive eye examination to verify normal acuity, ocular motility, stereoacuity, and ocular anatomy; none had undergoing any prior ocular surgery except for cataract surgery. We recruited 62 subjects of mean age 38.6±14.1 (range, 11–62) years from an ongoing study of strabismus who were determined to have unilateral SO palsy based upon significant ipsilesional reduction of maximum SO cross section on quasi-coronal MRI imaging. Subjects were excluded if there was a history of prior strabismus surgery, or if they could not cooperate for MRI. There were 32 men and 30 women. These subjects had initially presented with complaints of strabismus or diplopia. Eighteen cases of SO palsy were considered congenital, 20 traumatic, and 24 idiopathic. None had undergone strabismus surgery. The mean symptom duration of SO palsy was 57.7± 43.1 (range, 2–120) months. Each subject with SO palsy underwent complete ophthalmologic examinations including measurement of binocular misalignment using prism and cover testing and the Hess screen test. Subjective cyclodeviation was measured using double Maddox rods. Ocular versions with the tested eye in adduction were graded on a clinical scale of 0 to ±4, with 0 representing normal duction, −4 representing maximal underdepression or underelevation, and +4 representing maximal overdepression or overelevation.

MRI

A 1.5T General Electric Signa (Milwaukee, WI) scanner was used for imaging using T1, or T2 fast spin echo pulse sequences. Both sequences provide equivalent measurements. Technical details elsewhere published include use of a surface coil array (Medical

Advances, Milwaukee, WI) and fiber optic fixation target[14,19,20]. High-resolution (312 μm), quasi-coronal images of 2-mm thickness and matrix of 256×256 parallel to the long axis of the orbit were obtained in target controlled central gaze, supraduction, and infraduction for each eye. Because the scanned eye was centered on an afocal, monocularly viewed target that does not induce convergence, this procedure avoided confounding by strabismus.

Analysis

Image analysis was similar to published methods[21]. Digital MRIs were quantified using *ImageJ* (Rasband WS. ImageJ, U.S. National Institutes of Health, Bethesda, MD; http://rsb.info.nih.gov/ij/, 1997–2009, accessed February 2009). An ellipse was automatically fit to the SO cross section manually outlined in each image plane where it could be identified. The cross sectional area, and the major and minor axes of the ellipse, were automatically determined.

Statistical analysis

Main outcome measures were quantitative MRI morphometry, ocular versions, and binocular alignment as measured using prism-cover testing. Statistical analyses were performed using SPSS (ver. 16.0 for Windows; SPSS Science, Chicago, IL, USA). Significant effects of groups were evaluated using ANOVA, with subsequent pair-wise contrasts by unpaired *t*-tests and chi-square tests.

Results

All palsied SO muscles exhibited significant atrophy by MRI, but as hypothesized, there were two different general shapes of the atrophic SO cross sections. Fig. 1 illustrates MRI of whole orbital cross sections contrasting palsied and unaffected fellow SO bellies of two representative subjects, with a normal control for comparison, obtained at the anteroposterior location where the normal SO exhibits maximum cross section. The atrophic right SO in Fig. 1 (Top left) exhibits an elongated, narrowly oval cross section distinct from the rounder SO cross section of the unaffected left eye of the same subject (Fig. 1 Top right) that in turn is similar to both normal SO muscles of the control subject (Fig. 1 Bottom left and right). An ellipse fit to the SO cross section in Fig. 1 Top left would be long and narrow, which was considered to represent anisotropic atrophy. In contrast, the atrophic SO in Fig. 1 Middle left is uniformly so, exhibiting roughly circular cross section. An ellipse fit to the SO cross section in Fig. 1 Middle left would be nearly circular, which was considered to represent isotropic atrophy.

Initial qualitative classification of palsied SO morphology was based upon the foregoing two shapes. Twenty-six cases of SO palsy demonstrated isotropic atrophy of the SO belly as illustrated for 12 representative cases in Fig. 2. In 36 remaining cases, the atrophic SO belly exhibited an elongate shape typical of anisotropic atrophy, as illustrated for 12 representative cases in Fig. 3 in image plane 0, corresponding to the globe-optic nerve junction in central gaze. Despite individual variations in morphology and size for both normal and involved SO, in each case, the elongate shaped atrophy of SO belly is apparent.

The qualitative categorization of palsied SO morphology was then validated by quantitative morphometry of ellipses automatically fit to the SO cross sections. Figure 4 plots the mean length of major (top left) and minor (middle left) axes, and the mean area (bottom left) of the involved SO cross section in image planes throughout its anteroposterior extent in the orbit. Figure 4 top left demonstrates significant differences in major axis of the SO cross section among the anisotropic atrophy, isotropic atrophy, and normal control groups (P=0.001, ANOVA). This analysis confirms that in anisotropic atrophy group, the major axis of the SO cross section was modestly but significantly subnormal from image planes 1 to 5 posterior to the globe-optic nerve junction ($P < 0.05$ for all), but the major axis in the isotropic atrophy group was profoundly reduced throughout the entire length of the SO ($P < 0.0001$ for all) compared to normal. Figure 4 middle left shows significantly but similarly subnormal minor axes in the isotropic and anisotropic atrophy groups (P=0.001, ANOVA) throughout the entire SO length except the image plane 12 mm anterior to the globe-optic nerve junction. Figure 4 bottom left demonstrates more significant reduction in SO cross sectional area in the isotropic than anisotropic SO atrophy groups (P=0.001, ANOVA). This reduction was significant from 6 image planes posterior to 1 image plane anterior to the globe-optic nerve junction in the anisotropic atrophy group ($P < 0.05$ for all), but significantly subnormal throughout the entire length of the SO in the isotropic atrophy group ($P < 0.0001$ for all). Figure 4 illustrates that the major (top right) and minor axes (middle right), and the mean area (bottom right) of the SO cross sections of fellow eyes in both the anisotropic and isotropic SO atrophy groups were similar to normal ($P > 0.2$ for all).

Validity of the foregoing exploratory classification of SO cross sections was evaluated by post-hoc discriminant analysis based exclusively upon morphometry. We plotted the lengths of the major and minor axes of each palsied SO cross section in horizontal and vertical Cartesian coordinates, respectively. As seen in Figure 5, these points fell into two readily-separable groups based upon major axis length: those with major axis exceeding 3.9 mm were classified as having anisotropic atrophy (Fig. 5, circles), and those with major axis less than 3.9 mm were classified as having isotropic atrophy (Fig. 5, squares). There was no overlap between groups, despite variation in minor axis within each group.

The maximum cross sectional area for the palsied SO of the isotropic atrophy group was 5.81 ± 1.38 mm^2 (mean ± standard error, SE), which was less than those of the palsied SO of the anisotropic atrophy group at 8.21 ± 0.94 mm^2 (P=0.005). Both were considerably less than those of the normal SO in the normal control group (14.13 ± 0.89 mm^2, P=0.0001), and the unaffected fellow SO of the isotropic (17.01 ± 1.22 mm^2, P =0.001) and anisotropic atrophy groups (14.53 ± 0.94 mm^2, P=0.001). The isotropic atrophy group showed 66.2% reduction in SO cross sectional area, while the anisotropic atrophy group showed 43.5% reduction.

The maximum major axis for the palsied SO of isotropic atrophy group was 3.71 ± 0.39 mm^2, which was less than those of the palsied SO of anisotropic atrophy group at 5.54 ± 0.15 mm^2 (P=0.0146). Both were less than those of the normal control group (5.79 ± 0.18 mm^2, P=0.001, P=0.031, respectively), and the unaffected fellow SO of the isotropic (6.17 ± 0.20 mm^2, P=0.001, P=0.0121, respectively) and anisotropic atrophy groups (6.36 ± 0.21 mm^2, P=0.001, P =0.003, respectively).

The maximum minor axis for the palsied SO of the isotropic atrophy group was 2.11±0.21 mm^2, which was similar to those of the palsied SO of the anisotropic atrophy group at 2.05±0.11 mm^2 (P=0.693). Both were about a third less than those of the normal SO in the normal control group (2.99±0.12 mm^2, P=0.002, P=0.001, respectively), and the unaffected fellow SO of the isotropic (3.18±0.17mm^2, P=0.001) and anisotropic atrophy groups (3.14±0.16mm^2, P=0.001).

The SO belly volume was computed in planes ranging from 12 mm anterior to 12 mm posterior to the globe-optic junction (Fig. 6). The mean SO volume of the anisotropic atrophy group was 144.3±9.8mm^3, which was greater than those of the isotropic atrophy group at 97.5±16.8mm^3 (P=0.001). The SO belly volume of the anisotropic atrophy group was less than those of the normal control group (269.8±12.5 mm^3, P = 0.0001) and the unaffected fellow SO (261.1±6.6 mm^3, P=0.001). The SO belly volume of isotropic atrophy group was less than those of the normal control group (269.8±12.5 mm^3, P=0.0001) and the unaffected fellow SO (270.3±12.6 mm^3, P=0.0001). The isotropic atrophy group showed 66.3% reduction in SO volume, while the anisotropic atrophy group showed 44.5% reduction.

The SO palsy appeared to be congenital in 10 of 36 cases (28%) in the anisotropic atrophy group, which was a prevalence similar to the isotropic atrophic group (8 of 26, 31%). In the group with anisotropic SO atrophy, mean age of 39.9±17.4 (range, 14–61) years was not significantly different from the mean age of 26.3±13.1 (range, 11–66) years in the group with isotropic SO atrophy (P=0.783). Symptom duration in anisotropic atrophy group was 54.4±45.8 months, which was not significantly different from the isotropic atrophy group at 58.9±40.2 months (P = 0.292) after excluding congenital SO palsy because most congenital cases could not date symptom onset. Diplopia was reported by 44% (16 of 36) of subjects in the anisotropic atrophy group, which was not significantly different from the isotropic atrophy group at 54% (14 of 26, P=0.297). Table 1 showed the comparison of deviation and torsion between two atrophy groups. Hypertropia in central gaze, infraversion, and supraversion did not differ significantly between the two groups (P>0.05 for all). The variance in hypertropia involves contributions from both individual variations in SO anatomy, and differences in muscle function due to contractile change. Within individual subjects, the variation in comitance reflects muscle function. Thus, it is not inconsistent that the hypertropia in infraversion was greater than in central gaze in the anisotropic atrophy group, but not in the isotropic atrophy group (P=0.014). The anisotropic atrophy group exhibited 8.8±3.5° exclotorsion, which is greater than that of the isotropic atrophy group at 4.63±2.6° (P=0.032). The anisotropic atrophy group exhibited significantly greater underdepression in adduction than the isotropic atrophy group (P=0.0001), but there was no significant difference in over-elevation in adduction (P=0.608, Fig. 7).

Discussion

This study demonstrated by MRI two morphometrically distinct types of SO palsy based upon features of the cross section of the SO muscle belly: anisotropic, elongate atrophy, and isotropic, round atrophy. Subjects exhibiting anisotropic atrophy had greater hypertropia in

infraversion than central gaze, as well as greater exclyclotorsion did subjects exhibiting isotropic atrophy.

Neurogenic atrophy of extraocular muscles occurs reliably and rapidly following denervation[22,23]. Demer *et al*. reported atrophy of the midorbital cross section of the monkey SO following total trochlear neurectomy[18]. The gross cross section of the monkey SO was not uniformly reduced along the entire atrophic muscle length, but was redistributed anteriorly into the region of the trochlea normally occupied by tendon, so that the overall SO volume was only minimally reduced. The SO volume after intracranial trochlear neurectomy was 18% greater than on the intact side in one monkey, but was 12% less in second monkey and 26% less in third monkey. However, in the present study, the isotropic atrophy group showed a significant 66% reduction in SO volume, and the anisotropic atrophy group showed 44% reduction. The volume reduction in the palsied human SO was greater than those in the monkey study. In the present study, the cross sectional area of the palsied SO was reduced at all image planes evaluated. These differences might be due to the differences of etiology, duration of palsy, and species. The durations of SO palsy were long and quite variable, which might have masked possible early secular effects on SO shape.

In context of new anatomical understanding of the intramuscular SO innervation, we interpret the data in context of compartmentalization. The elongate, oval shaped SO belly in the anisotropic atrophy group is consistent with palsy of only one compartment, while the round, uniform SO belly in the isotropic atrophy group is consistent with palsy of both compartments. The anisotropic atrophy group would presumably maintain function in part of the SO. However, we cannot differentiate medial compartment palsy from lateral compartment palsy based on SO cross section morphology with current MRI technique. Thus, the anisotropic atrophy group could presumably include both cases of selective medial and other cases of selective lateral compartment palsy; the clinical presentation of the resulting group would be mixed, unless one compartment were selectively vulnerable to pathology. Selective compartmental vulnerability, while of course unproven in SO, has been suggested for lateral rectus by the frequent occurrence of palsy of only the superior compartment of that extraocular muscle, which represents about 30% of cases of lateral rectus weakness[3]. Heterogeneity of medial vs. lateral compartmental SO palsy in the group with anisotropic atrophy is one possible explanation why subjects exhibiting anisotropic atrophy both had greater hypertropia in infraversion than central gaze, as well as greater exclyclotorsion did subjects exhibiting isotropic atrophy. But it is also likely that abnormal SO function is associated with compensatory responses throughout the extraocular muscle compartments of both orbits. Similar widespread and sometimes paradoxical behaviors have been observed by MRI during vertical fusional vergence in normal people, including relaxation of the SO lateral compartment of the infraducting eye[7].

In both uniform and non-uniform SO palsies, the size of SO belly varied for several possible reasons. First, the size of the pre-lesion SO belly might have varied among subjects. Second, the pre-lesion distribution of muscle fibers between the medial and lateral compartments might have been varied among subjects. Finally, the causative pathology may have varied.

In the isotropic atrophy group, three subjects showed very small SO cross sectional area, and all of these had congenital SO palsy. However, very small, round SO cross section was not universally found in congenital SO palsy In the anisotropic atrophy group, subjects 3, 5, 7, and 9 had the congenital palsy and anisotropic SO atrophy, albeit with cross section no smaller than other subjects with anisotropic atrophy. Perhaps this reflects differences in the etiology of atrophy, perhaps a structural abnormality of myoblast migration in congenital SO palsy, and abnormal innervation in acquired SO palsy. Ozkan *et al*. observed no significant differences in mean SO width and cross sectional area between cases of congenital and acquired SO palsy[15]. Sato et al. reported smaller SO belly volume in congenital than acquired SO palsy, but no significant effect of age on muscle atrophy in congenital and acquired SO palsies [15]. In acquired SO palsy, Sato found no relationship between duration of palsy and severity of SO atrophy. This finding is consistent with Demer *et al*.'s report of rapid completion of neurogenic SO atrophy in monkey after no more than 5 weeks post-denervation [24]. However, none of the foregoing studies classified SO atrophy morphometrically.

Although many variable types of SO palsy have been proposed by earlier authors, classification based on the shape of SO cross section is novel. A recent study of 50 patients who showed definite SO atrophy on MRI found that only 70% fulfilled the entire three-step test [25]. This implies that the three-step test has only 70% sensitivity for detection of SO atrophy. And another study demonstrated that only about half of subjects with positive three-step tests exhibit SO atrophy, [26] implying only about 50% specificity of the test. Therefore, MRI is probably more reliable than conventional clinical methods for distinguishing actual SO palsy from masquerading conditions. Imaging may be clinically important if the etiologic diagnosis has therapeutic or management implications.

The present study demonstrates two distinctive morphologies of SO atrophy associated with SO palsy that correlated with different clinical features, and suggests that the compartmental nature of SO function should be considered to understand the highly diverse presentations of SO pathology. Further study is needed to investigate possible differences in response of the two morphological patterns of SO palsy to surgical treatment.

Acknowledgments

Funding/Support: This study was supported by grants to JLD from the U.S. Public Health Service (NEI grant EY08313), Washington, DC, and an unrestricted grant from Research to Prevent Blindness, New York, NY. SYS was supported by the Department of Ophthalmology and Visual Science, Seoul St. Mary's Hospital, College of Medicine The Catholic University of Korea, Seoul, South Korea. These entities were not involved in reporting or interpretation of the data.

Dr. Shin was supported during this study by Department of Ophthalmology and Visual Science, Seoul St. Mary's Hospital, College of Medicine, The Catholic University of Korea, Seoul, South Korea, where she is again located full time.

References

1. Demer JL. Compartmentalization of extraocular muscle function. Eye (Lond). 2014 Oct 24.10.1038/eye.2014
2. Clark RA, Demer JL. Differential compartmental function of medial rectus muscle during conjugate and converged ocular adduction. J Neurophysiol. 2014; 112(4):845–855. [PubMed: 24848474]

3. Clark RA, Demer JL. Lateral rectus superior compartment palsy. Am J Ophthalmol. 2014; 157(2): 479–487. [PubMed: 24315033]
4. da Silva Costa RM, Kung J, Poukens V, Yoo L, Tychsen L, Demer JL. Intramuscular innervation of primate extraocular muscles: Unique compartmentalization in horizontal recti. Invest Ophthalmol Vis Sci. 2011; 52(5):2830–2836. [PubMed: 21220556]
5. Peng M, Poukens V, da Silva Costa RM, Yoo L, Tychsen L, Demer JL. Compartmentalized innervation of primate lateral rectus muscle. Invest Ophthalmol Vis Sci. 2010; 51(9):4612–4617. [PubMed: 20435590]
6. Clark RA, Demer JL. Differential lateral rectus compartmental contraction during ocular counter-rolling. Invest Ophthalmol Vis Sci. 2012; 53(6):2887–2896. [PubMed: 22427572]
7. Demer JL, Clark RA. Magnetic resonance imaging demonstrates compartmental muscle mechanisms of human vertical fusional vergence. J Neurophysiol. 2015 Jan 14.10.1152/jn.00871.2014
8. Shin A, Yoo L, Chaudhuri Z, Demer JL. Independent passive mechanical behavior of bovine extraocular muscle compartments. Inv Ophtalmol Vis Sci. 2012; 53(13):8414–8423.
9. Shin A, Yoo L, Demer JL. Viscoelastic characterization of extraocular z-myotomy. Inv Ophtalmol Vis Sci. 2015; 56(1):243–251.
10. Shin A, Yoo L, Demer JL. Biomechanics of superior oblique Z-tenotomy. J AAPOS. 2013; 17(6): 612–617. [PubMed: 24321425]
11. Shin A, Yoo L, Demer JL. Independent active contraction of extraocular muscle compartments. Inv Ophtalmol Vis Sci. 2015; 56(1):199–206.
12. Pihlblad MS, Demer JL. Hypertropia in unilateral isolated abducens palsy. J AAPOS. 2014; 18(3): 235–240. [PubMed: 24924275]
13. Horton JC, Tsai RK, Truwit CL, Hoyt WF. Magnetic resonance imaging of superior oblique muscle atrophy in acuired trochlear nerve palsy [letter]. Am J Ophthalmol. 1990; 110(3):315–316. [PubMed: 2396662]
14. Demer JL, Miller JM. Magnetic resonance imaging of the functional anatomy of the superior oblique muscle. Invest Ophthalmol Vis Sci. 1995; 36(5):906–913. [PubMed: 7706039]
15. Ozkan SB, Aribal ME, Sener EC, Sanac AS, Gurcan F. Magnetic resonance imaging in evaluation of congenital and acquired superior oblique palsy. J Pediatr Ophthalmol Strabismus. 1997; 34(1): 29–34. [PubMed: 9027677]
16. Sato M, Yagasaki T, Kora T, Awaya S. Comparison of muscle volume between congenital and aquired superior oblique palsies by magnetic resonance imaging. Jpn J Ophthalmol. 1998; 42(6): 466–470. [PubMed: 9886737]
17. Kono R, Demer JL. Magnetic resonance imaging of the functional anatomy of the inferior oblique muscle in superior oblique palsy. Ophthalmology. 2003; 110(6):1219–1229. [PubMed: 12799250]
18. Demer JL, Poukens V, Ying H, Shan X, Tian J, Zee DS. Effects of intracranial trochlear neurectomy on the structure of the primate superior oblique muscle. Invest Ophthalmol Vis Sci. 2010; 51(7):3485–3493. [PubMed: 20164458]
19. Demer, JL.; Miller, JM. Orbital Imaging in strabismus surgery. In: Rosenbaum, AL.; Santiago, AP., editors. Clinical Strabismus Management: Principles and Techniques. Philadelphia: Saunders; 1999.
20. Demer JL, Dusyanth A. T2-weigted fast spin-echo magnetic resonance imaging of extraocular muscles. J AAPOS. 2011; 15(1):17–23. [PubMed: 21397801]
21. Demer JL, Clark RA, Kono R, Wright W, Velez F, Rosenbaum AL. A 12 year, prospective study of extraocular muscle imaging in complex strabismus. J AAPOS. 2002; 6(6):337–347. [PubMed: 12506273]
22. Porter JD, Bruns LA, McMahan EJ. Denervation of primate extraocular muscle. Invest Ophthalmol Vis Sci. 1989; 30(8):1894–1908. [PubMed: 2759804]
23. Baker RS, Millett AJ, Young AB, Markesbery WR. Effects of chronic denervation on the histology of canine extraocular muscle. Invest Ophthalmol Vis Sci. 1982; 22(6):701–705. [PubMed: 7076415]

24. Demer JL, Poukens V, Ying H, Shan X, Tian J, Zee DS. Effects of intracranial trochlear neurectomy on the structure of the primate superior oblique muscle. Invest Ophthalmol Vis Sci. 2010; 51(7):3485–3493. [PubMed: 20164458]
25. Manchandia A, Demer JL. Sensitivity of the three-step test in diagnosis of superior oblique palsy. J AAPOS. 2014; 18(6):567–571. [PubMed: 25459202]
26. Demer JL, Clark RA, Kung J. Functional imaging of human extraocular muscles in head tilt dependent hypertropia. Inv Ophthalmol Vis Sci. 2011; 52(6):3023–3031.

Biographies

Sun Young Shin, MD, received her MD from Hanyang University Medical School, Seoul, Republic of (South) Korea in 1997, where she also completed her residency in the Department of Ophthalmology with subsequent sub-specialty training on the pediatric ophthalmology and strabismus. Dr. Shin is a former Assistant Professor at the Department of Ophthalmology, College of Medicine, Hanyang University from 2005 to 2007. She is currently an Associate Professor at the Department of Ophthalmology and Visual Science at The Catholic University of Korea, Seoul, South Korea.

Joseph L. Demer, M.D., Ph.D. is Division Chief and holds the Leonard Apt Professorship of Pediatric Ophthalmology and Strabismus at the Stein Eye Institute, David Geffen School of Medicine at UCLA. He is Professor of Neurology and chairs the EyeSTAR Residency-PhD Program. In 2003, Dr. Demer received the Friedenwald Award from ARVO, and a Recognition Award from the Alcon Research Institute in 2004, for his work on the extraocular muscles and orbital connective tissues.

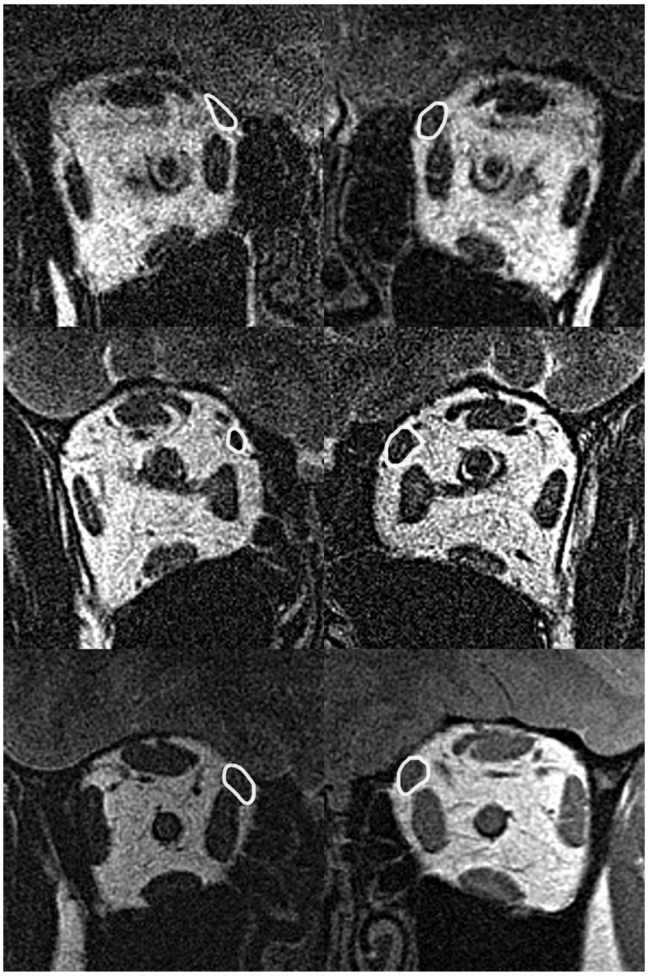

Fig. 1.

Quasi-coronal MRI of right (left column) and left (right column) orbits in superior oblique (SO) palsy. Each SO cross section is outlined in white. Top row - Subject with right unilateral anisotropic superior oblique (SO) atrophy manifesting elongate, oval shape compared to the unaffected left SO. Middle row – Subject with right unilateral isotropic SO atrophy group manifesting uniform, circular reduction in right cross section compared to the unaffected fellow eye. Bottom row – Normal control subject has similar SO cross sections in both orbits.

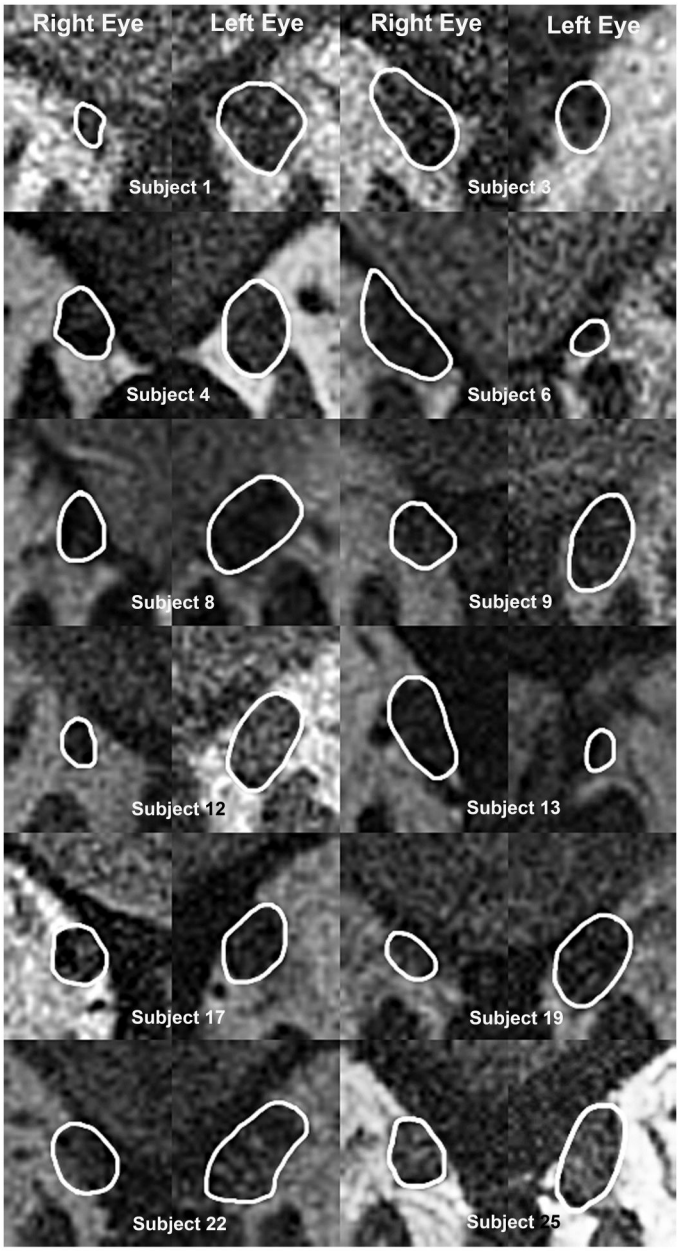

Fig. 2.

Quasi-coronal MRI in unilateral superior oblique (SO) palsy cropped to show SO muscles exhibiting isotropic atrophy, and corresponding normal fellow muscles.

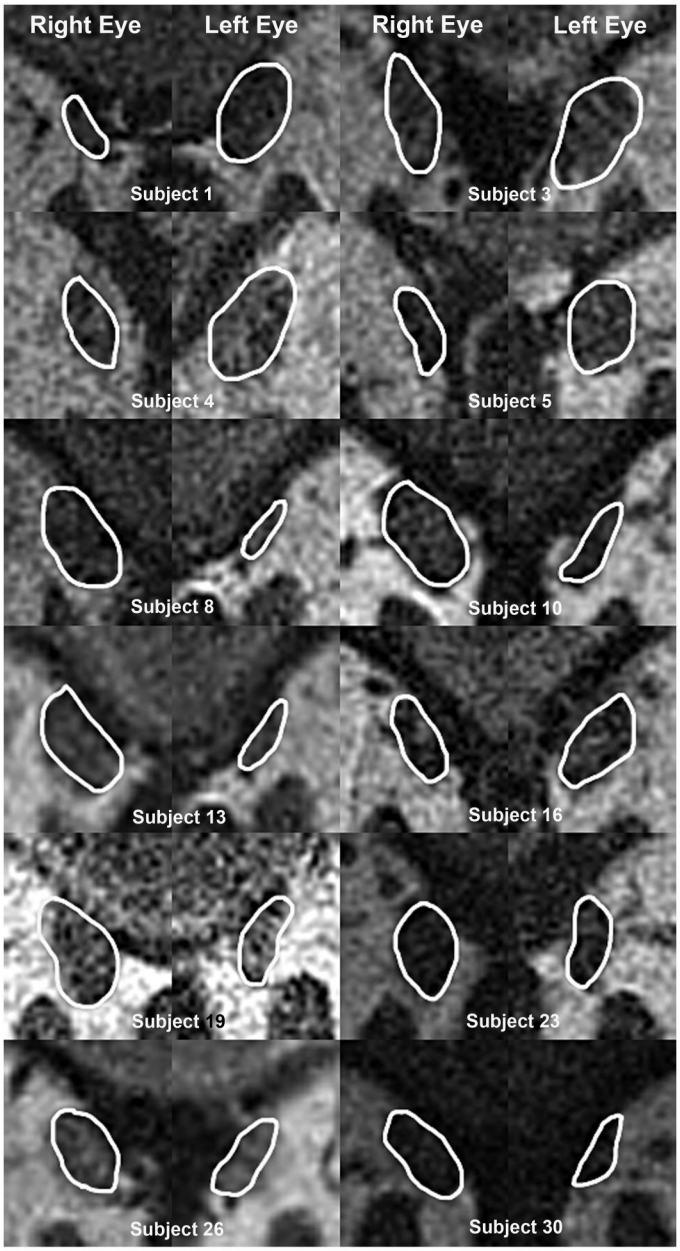

Fig. 3.

Quasi-coronal MRI cropped to show superior oblique muscles exhibiting anisotropic atrophy in superior oblique palsy, and corresponding normal fellow muscles.

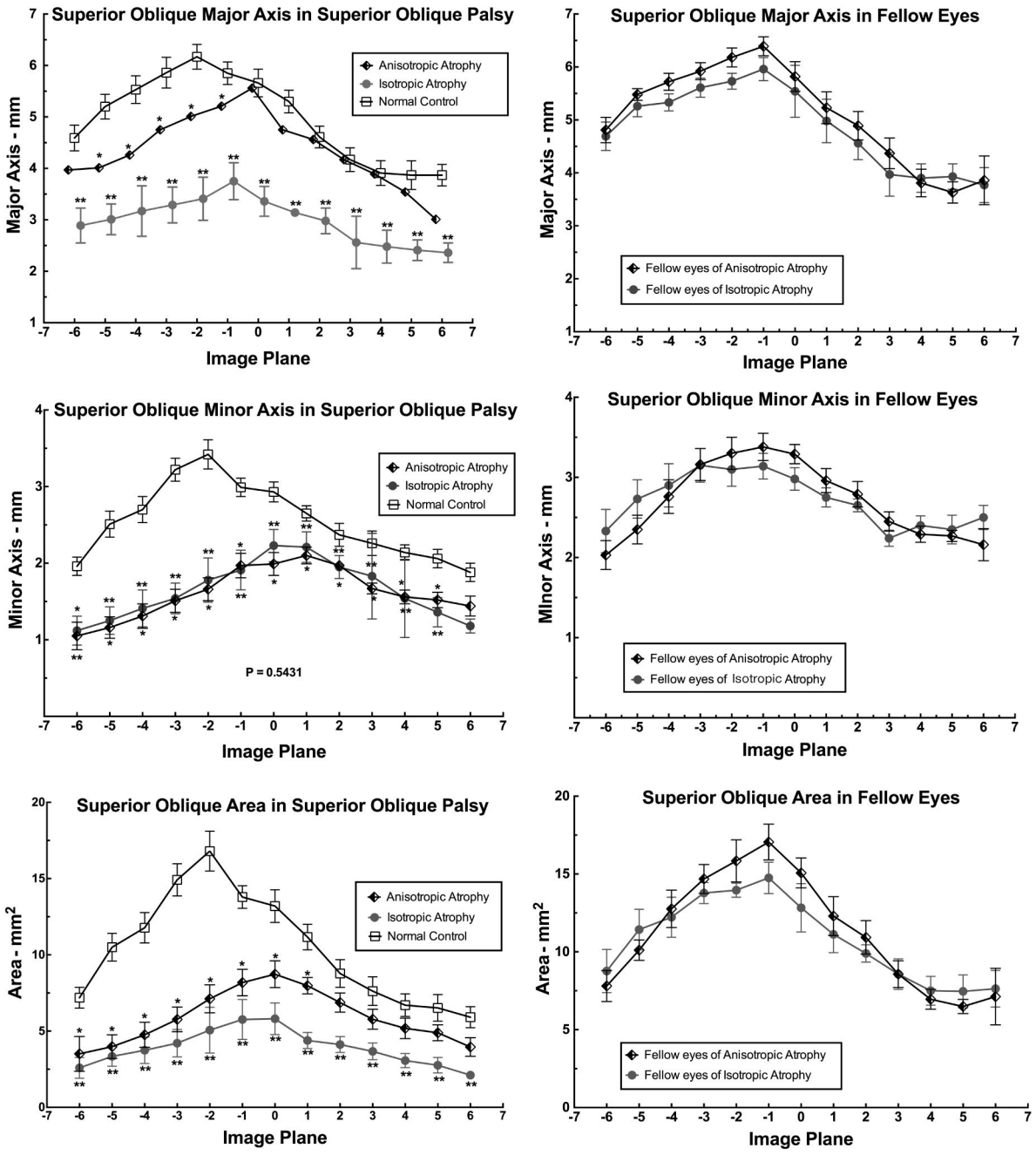

Fig. 4.

Major and minor axes of the superior oblique (SO) cross section in SO palsy exhibiting isotropic and anisotropic SO atrophy, and in normal control subjects. Image planes are 2 mm thick image and numbered positively anterior and negatively posterior to zero at the globe-optic nerve junction. Significant differences from normal are indicated by single and double asterisks at the 0.05 and 0.01 levels, respectively, by unpaired t testing.

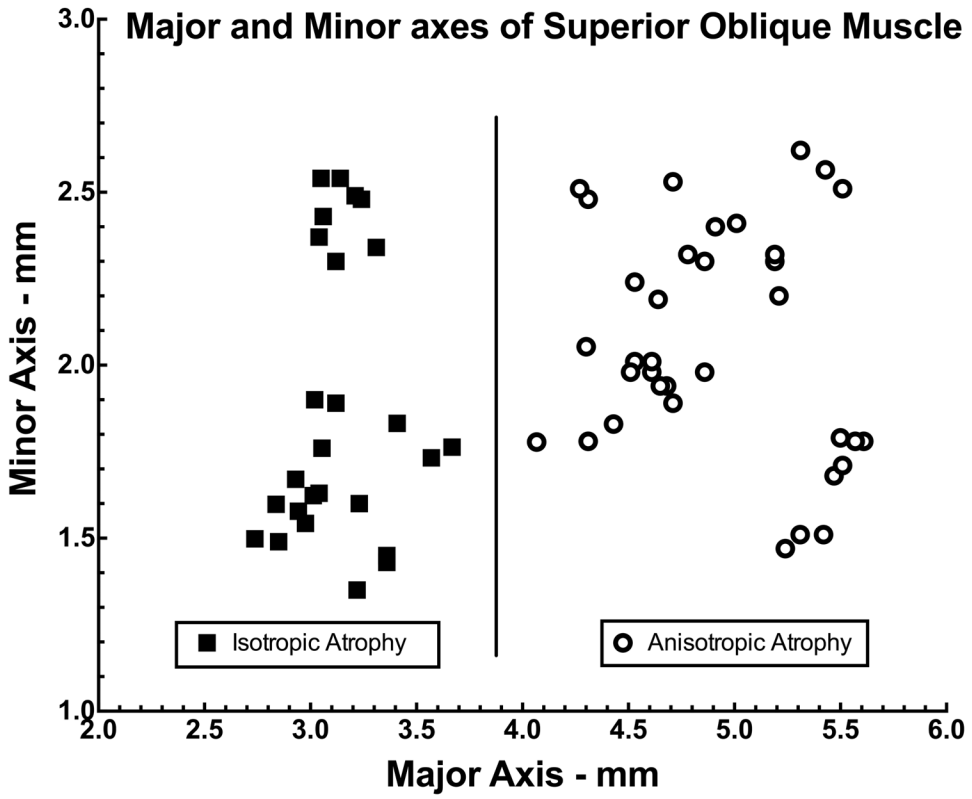

Fig. 5.

Discriminant analysis of major and minor axes of the palsied superior oblique (SO) belly at in quasi-coronal image planes at the globe-optic nerve junction (image plane 0) in 62 cases of unilateral SO palsy. Each symbol indicates one case. Two morphometric groups were discriminable. Cases clustered in the left half of the graph exhibited isotropic atrophy (squares), while cases clustered in the right half exhibited anisotropic atrophy (circles).

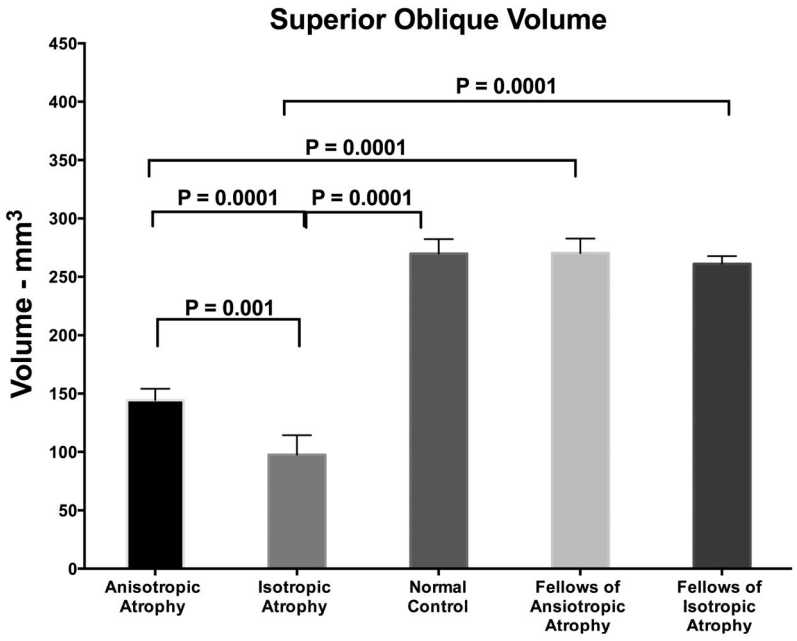

Fig. 6.

Superior oblique (SO) volume in unilateral SO palsy manifesting anisotropic and anisotropic atrophy, and in normal control cases. Error bars indicate standard error of the mean.

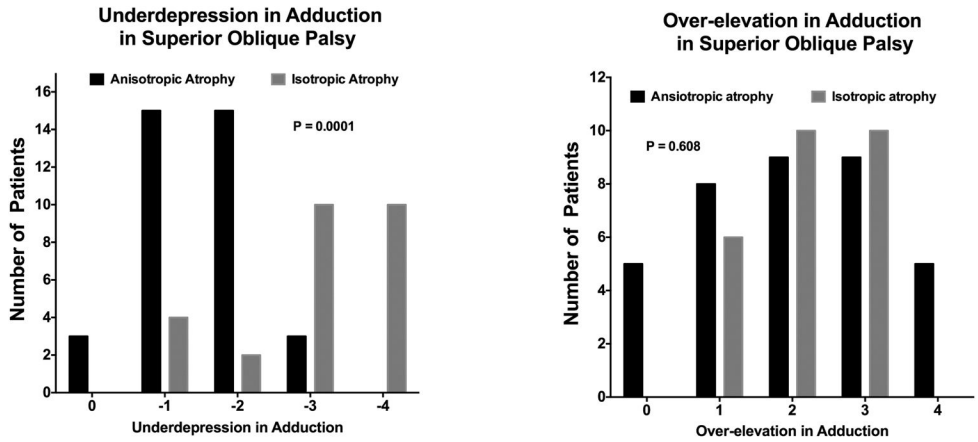

Fig. 7.

Underdepression in adduction (left) and over-elevation in adduction (right) in superior oblique (SO) palsy. Values are rated on a scale of −4 underaction to +4 overaction, with normal defined as zero. Chi-square testing demonstrated significantly more underdepression in adduction in isotropic than anisotropic SO atrophy.

Table 1

Binocular Alignment Unilateral Superior Oblique Atrophy

		Anisotropic Atrophy (n=36)	Isotropic Atrophy (n=26)	P value
Age (years)		39.9±17.4	26.3±13.1	0.783
Hypertropia (Δ)	Central Gaze	14.1±7.4	13.6±7.1	0.899
	Sursumversion	9.6±7.6	9.3±8.7	0.914
	Infraversion	16.7±13.7	6.4±4.8	0.048
Incomitance (Δ) of Hypertropia	Central Minus Sursumversion	3.8±2.9	3.1±6.3	0.956
	Central Minus Infraversion	−4.6±7.7	6.3±5.7	0.014
	Lateral	10.6±7.5	10.1±5.7	0.916
	Right Minus Left Head Tilt	10.9±6.5	14.3±8.1	0.586
Excyclortorsion (degrees)		8.8±3.5	4.3±2.6	0.032